Synthesis and structure-activity relationships of novel hybrid ferrocenyl compounds based on a bicyclic core skeleton for breast cancer therapy

Changhao Li, Chu Tang, Zhiye Hu, Chenxi Zhao, Chenlu Li, Silong Zhang, Chune Dong, Hai-Bing Zhou, Jian Huang

PII: S0968-0896(16)30343-1
DOI: http://dx.doi.org/10.1016/j.bmc.2016.05.019
Reference: BMC 13003

To appear in: *Bioorganic & Medicinal Chemistry*

Received Date: 1 April 2016
Revised Date: 12 May 2016
Accepted Date: 12 May 2016

Please cite this article as: Li, C., Tang, C., Hu, Z., Zhao, C., Li, C., Zhang, S., Dong, C., Zhou, H-B., Huang, J., Synthesis and structure-activity relationships of novel hybrid ferrocenyl compounds based on a bicyclic core skeleton for breast cancer therapy, *Bioorganic & Medicinal Chemistry* (2016), doi: http://dx.doi.org/10.1016/j.bmc.2016.05.019

Synthesis and structure-activity relationships of novel hybrid ferrocenyl compounds based on a bicyclic core skeleton for breast cancer therapy

Changhao Li [a], Chu Tang [b], Zhiye Hu [b], Chenxi Zhao [a], Chenlu Li [b], Silong Zhang [b], Chune Dong [b], Hai-Bing Zhou [b,*], Jian Huang [a,*]

[a] *College of Life Sciences, Wuhan University, Wuhan 430072, China*

[b] *Hubei Provincial Key Laboratory of Developmentally Originated Disease, Wuhan 430071, China; Key Laboratory of Combinatorial Biosynthesis and Drug Discovery (Wuhan University), Ministry of Education; Wuhan University School of Pharmaceutical Sciences, Wuhan 430071, China*

**Correspondence to: Hai-Bing Zhou, Tel 862768759586, zhouhb@whu.edu.cn; Jian Huang, Tel 86276875358, jianhuang@whu.edu.cn.*

ARTCLE INFO

Article history:
Received
Received in revised from
Accepted
Available online

Keywords:
Breast cancer
SERMs
HDACi
Ferrocenyl

ABSTRACT

Breast cancer is the most frequent cancer in women worldwide, and incidence is increasing year by year. Although current selective estrogen receptor modulators (SERMs) have clear advantages in the treatment of hormone-responsive breast cancer, they are ineffective for ER(-). In this study, we describe the design and synthesis of a series of dual-acting estrogen receptor (ER) and histone deacetylase (HDAC) inhibitors with incorporation of the ferrocenyl moiety, leading to novel hybrid ferrocenyl complexes (FcOBHS-HDACis) for breast cancer therapy. It is worth to note that these ferrocenyl conjugates could not only potently inhibit HDACs and the proliferation of ERα positive (ER(+)) breast cancer cells (MCF-7), but also show significant antiproliferative effect on ER(-) breast cancer cells (MDA-MB-231). Thus, the FcOBHS-HDACi conjugates represent a novel approach to the development of efficiently dual-acting agents for treatment of breast cancer.

1. Introduction

Breast cancer is the most frequent cancer in women worldwide, and incidence is increasing year by year. Approximately 15% of women are diagnosed with breast cancer in the reproductive age,[1] and it is the leading cause of cancer death in women between 35 and 55 years of age.[2, 3] Estrogen receptors (ERs, comprising of two subtypes ERα and ERβ) and endogenous estrogens play essential roles in the growth of breast tumors.[4] Some selective estrogen receptor modulators (SERMs) such as tamoxifen or raloxifene, which act at the breast as anti-estrogens, are widely used in the clinic for the treatment of this disease.[5-7] Although certain SERMs are useful for the treatment of breast cancer, unfortunately, an undesired side effect severely limits their therapeutical use. For instance, tamoxifen is the first clinically used SERM for treatment of breast cancer,[8, 9] however, due to the partial estrogenic activity on the endometrium, the clinical use is associated with uterine hypertrophy and an increased risk of endometrial cancer; in addition, tamoxifen therapy is ineffective for ER(-) breast cancer.[10-12] It is thus evident that there is a need for new ER ligands that are more effective in ER(-) breast cancer. To address the need of disease-modifying drugs for breast cancer, in recent years, new strategies have been devised in medicinal chemistry, one that has received significant attention is to develop bivalent agents through combining two bioactive drugs into a single molecule.

In the field of breast cancer, this strategy involved linking a potent ER ligand to a second component, such as an antimitotic agent (E_2-paclitaxel conjugate **1**),[13] antimetabolite agent (E_2-nucleoside conjugate **2**),[14] alkylating agent (E_2-chlorambucil conjugate **3**),[15] steroid sulfatase agent (Estrone 3-*O*-sulfamate **4**),[16] tubulin agent (dual ER-tubulin agent **5**),[17] and aromatase agent (dual ER-aromatase agent **6**) *etc.*[18-21] Despite important

progress in this area, there is still room for improvement regarding dual-acting hybrids, because many bioactive hybrids show extremely low ER binding affinity or lack target-tissue selectivity.[22] Therefore, numerous efforts have been done to develop new bioactive hybrid compounds with higher ER binding affinity, target-tissue selectivity and lower inherent toxicity.

In another aspect, histone deacetylases (HDACs) have recently emerged as important targets for cancer therapy, including breast cancer.[21, 23] In particular, HDAC may be a potential target for therapeutic intervention in the treatment of ER negative breast cancers.[24, 25] These evidences suggest simultaneous ER and HDAC inhibition could be a promising approach in breast cancer therapy. Indeed, recent observations have shown that dual-acting ER ligand-HDACi conjugates have an improved *in vitro* therapeutic index and potent anti-cancer activity;[26-29] yet, they retain some disadvantages. For instance, most benzothiophene scaffold-based hybrid HDAC inhibitors (*e.g.*, compound **7**, Figure 2) show little effect on ER transcriptional activity,[29] ethynylestradiol-HDACi conjugates (*e.g.*, compound **8**, Figure 2) retain the ERα agonist activity of their parent compound EED and Tam-HDACi conjugates (*e.g.*, compound **9**, Figure 2) are toxic to the healthy cells.[26]

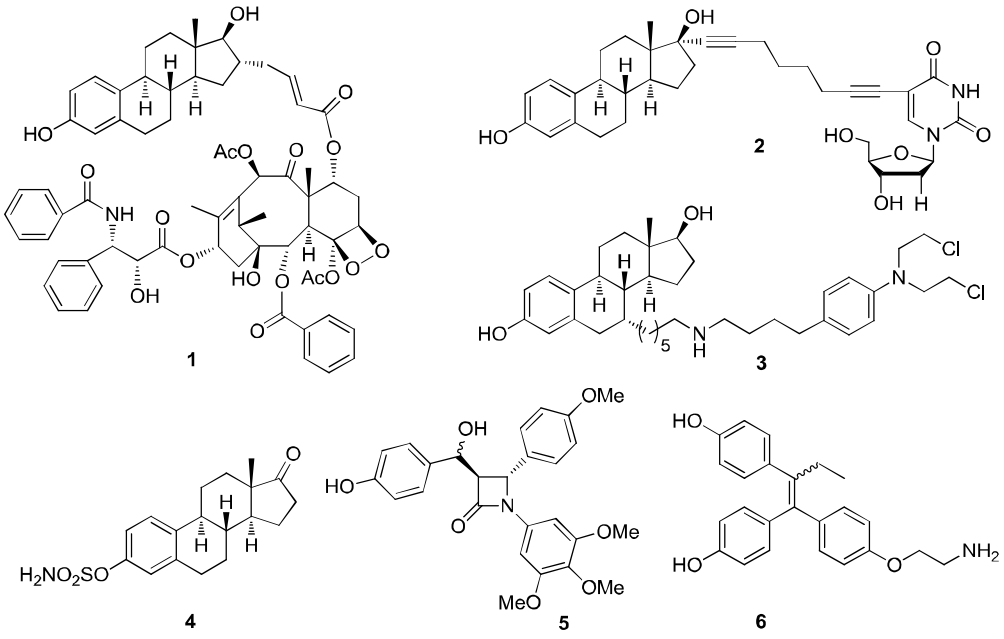

Figure 1 Currently referenced dual-acting ER ligand conjugates

As part of our long-term interest in the development of ligands for the ERs having novel structures and activities, we have prepared a novel series of three-dimensional ER ligands based on 7-oxabicyclo[2.2.1]hept-5-ene core, in which OBHS (5,6-bis-(4-hydroxyphenyl)-7-oxabicyclo[2.2.1]hept-5-ene-2-sulfonic acid phenyl ester, compound **10**, Figure 2) was one of the most promising antagonist compounds.[30-35] Recently, our research group has chosen HDACi as the second component and synthesized dual-acting OBHS-HDACi conjugates.[35] Two of these bifunctional conjugates (*e.g.* compounds **11** and **12**, Figure 2) exhibited good ER binding affinity, excellent ERα antagonistic activity and significant anti-proliferative effect on ERα(+) breast cancer cells (MCF-7); moreover, they had no toxicity towards normal cells. It should be emphasized that HDACi unit of conjugates possessing the suberic acid group rather than hydroxamate exhibits greater activity.[35, 36] Unfortunately, these bifunctional hybrid OBHS-HDACi conjugates showed very weak anti-proliferative effect on ER(-) breast cancer (MDA-MB-231, $IC_{50} > 50$ μM). Our aim now is to extend therapeutic effectives of these OBHS-HDACi conjugates that would produce a powerful antiproliferative effect on both ER(+) and ER(-) breast cancer cells.

In recent years, bioorganometallic chemistry has attracted active interest in medicinal chemistry, and numerous classes of organometallic compounds have been found application in drug design. Specifically, ferrocene (Fc) has generated much interest

in cancer therapeutics literature. Ferrocenyl derivatives usually are not toxicity and lipophilic, and have good redox properties.[37-39] Several ferrocenyl compounds display interesting antitumor activity, and the hydroxyferrocifen, the mostly studied that selectively targets breast cancer and shows a strong antiproliferative effect on both ER(+) and ER(-) breast cancer cells.[40] Furthermore, there has been a number of examples of other ferrocene containing compounds that also exhibit great activity against ER(-) breast cancer cells.[41-43] At the same time, our group has reported that incorporation of the ferrocenyl unit into OBHS can lead to OBHS complexes (termed FcOBHS) showing significant antiproliferative effect on both ER(+) and ER(-) breast cancer cells.[32]

In order to extend therapeutic effectives of OBHS-HDACi conjugates above for both ER(+) and ER(-) breast cancer cells, in this paper, we report a new family of ferrocene complexes (termed FcOBHS-HDACi conjugate, Figure 3) based on OBHS-HDACi core scaffold, with two strategies to introduce the ferrocenyl group into the OBHS-HDACi skeleton. First, we introduced the ferrocenyl group on the phenyl ring of sulfonate unit (Series I); the second approach involved substituting one phenol ring on C5 or C6 with ferrocenyl group (Series II). Subsequently, the biological activity of these FcOBHS-HDACi conjugates was studied. It has been observed that these dual-acting conjugates showed moderate binding affinity for ERs and strong inhibition activity towards HDACs. Several molecules retain great activity of the parent compound against ER(+) breast cancer cells (MCF-7), and more importantly, could effectively inhibit the proliferation of ER(-) breast cancer cells (MDA-MB-231). While chain length of HDACi unit is a major factor for their inhibitory activities, and the conjugates presenting that a shorter rather than longer chain length tend to be more active, especially those with suberic acid unit. These results suggest that conjugation of ferrocenyl group to estrogen modulators could improve therapeutic activity.

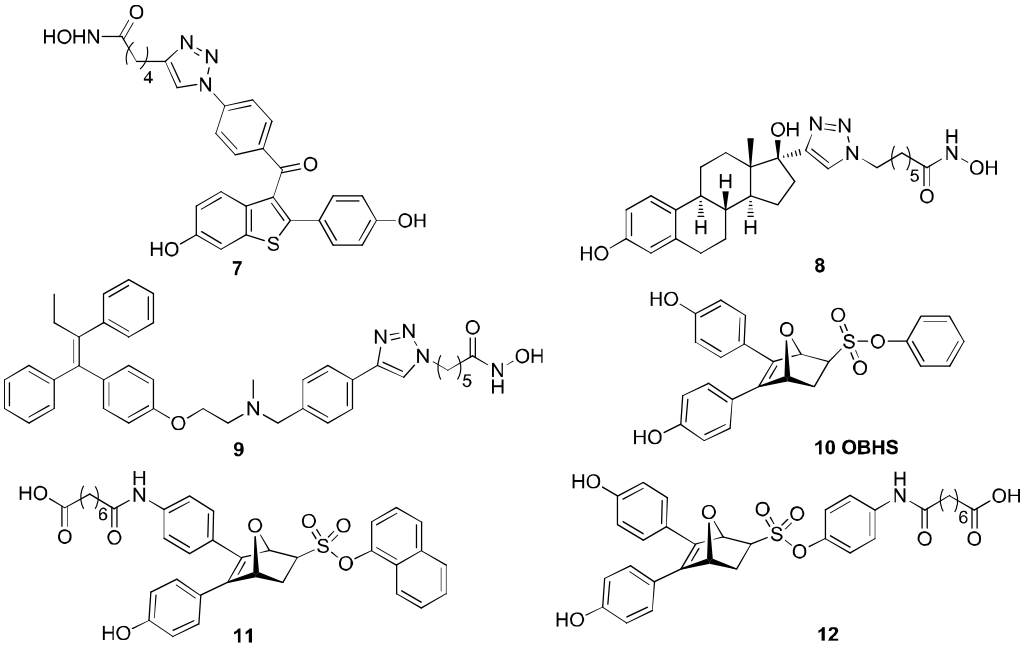

Figure 2 Structures of dual-acting ER ligand-HDACi conjugates

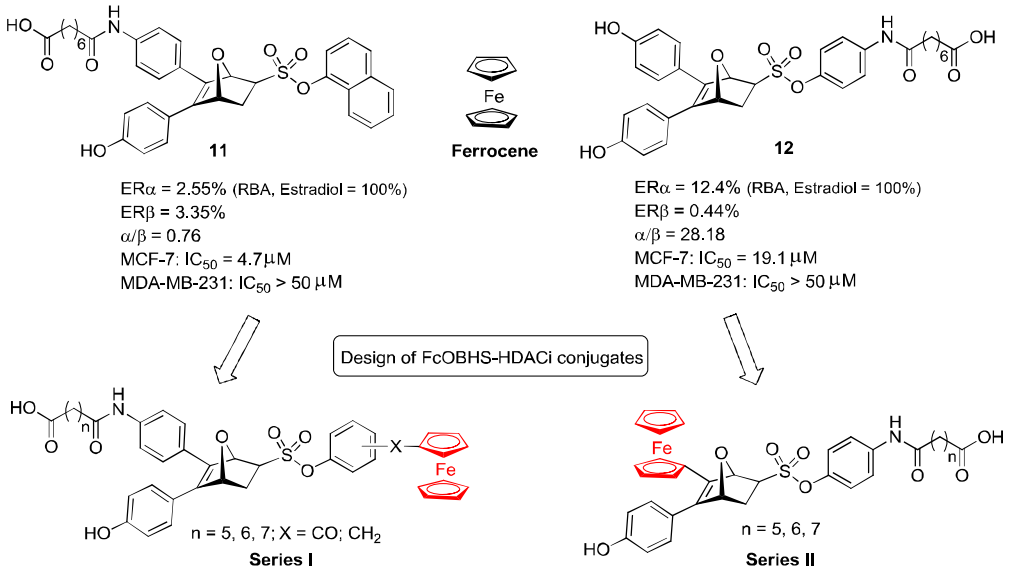

Figure 3 Design of dual-acting FcOBHS-HDACi conjugates

2. Results and Discussion

2.1. Chemical Synthesis

All designed FcOBHS-HDACi conjugates were prepared by a Diels-Alder cycloaddition of furan derivatives **19a-c** or 3-ferrocenyl-4-(4-hydroxyph-enyl) furan **29** with various dienophiles (Schemes 1-3). The important intermediates, furan derivatives **19a-c** and **29**, were prepared according to our previously reported methodology (Schemes 1 and 3).[32, 35] The synthesis of ferrocenyl vinyl sulfonates **24a-c** was accomplished by three steps: firstly, the Fc **20** reacted with 3-methoxybenzoyl chloride **21a**, 4-methoxybenzoyl chloride **21b** or 4-methoxybenzyl alcohol **21c** in the presence of different acid catalysts ($AlCl_3$ for **22a-b**, CF_3COOH for **22c**) to afford the corresponding ferrocenyl substituted products **22a-c**. Subsequent *O*-demethylation with boron tribromide afforded phenolic products **23a-c**, which were then reacted with 2-chloroethanesulfonyl chloride in the presence of Et_3N gave the ferrocenyl dienophiles **24a-c** (Scheme 2A).[32]

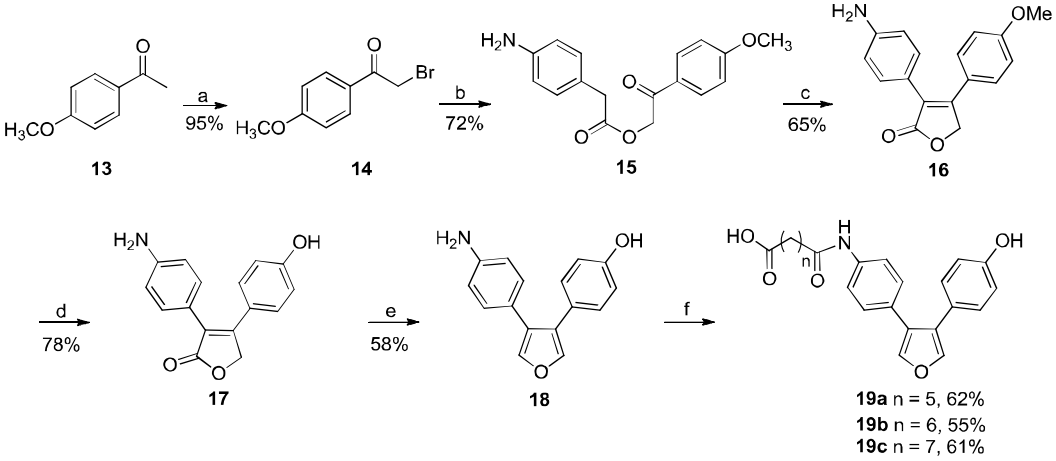

Scheme 1 Synthesis of furan derivatives **19a-c**. Reagents and conditions: (a) NBS (1.2 equiv.), *p*-TsOH (0.2 equiv.), $CHCl_3$, rt, 12 h; (b) 4-aminophenylacetic acid, Et_3N, CH_3CN, rt, 12 h; (c) NaH, DMSO, rt, 3 h; (d) BBr_3, CH_2Cl_2, -20 °C, 12 h; (e) DIBAL-H, THF, -78 °C, 8 h; (f) pimelic anhydride for **19a**; suberic anhydride for **19b**; azelaic anhydride for **19c**, THF, rt, 2 h.

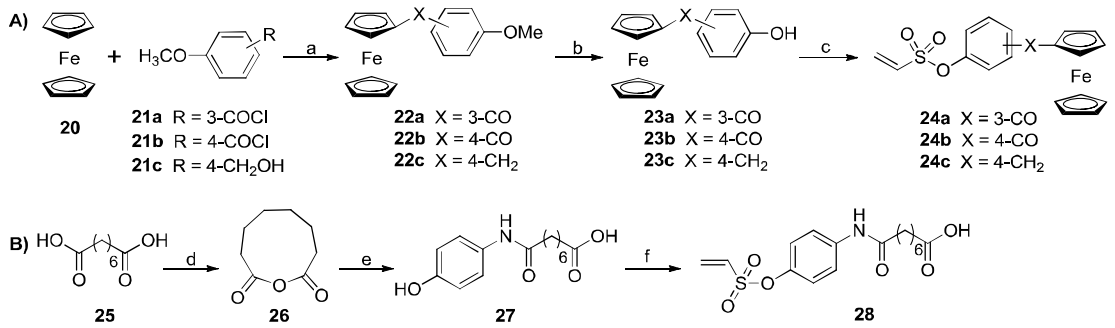

Scheme 2 Synthesis of dienophiles **24a-c** and **28**. Reagents and conditions: (a) $AlCl_3$ for **22a-b**; CF_3COOH for **22c**, CH_2Cl_2, 0 °C, 1 h; (b) BBr_3, CH_2Cl_2, -20 °C, 12 h; (c) 2-chloroethanesulfonyl chloride, Et_3N, CH_2Cl_2, 0 °C, 12 h; (d) acetic anhydride, 150 °C, 1 h; (e) 4-aminophenol, THF, rt, 1 h; (f) 2-chloroethanesulfonyl chloride, Et_3N, THF, 0 °C, 12 h.

The vinyl sulfonate **28** was prepared following a previously reported route (Scheme 2B).[35] We used suberic acid **25** as the starting material, which was treated with acetic anhydride to give suberic anhydride **26**.[44] Then, suberic anhydride **26** was condensed with 4-aminophenol to generate compound **27**, which was subsequently reacted with 2-chloroethanesulfonyl chloride to yield the vinyl sulfonate **28**. The synthesis of FcOBHS-HDACi conjugates was carried out successfully to give the first three conjugates (**31a-c**, linker length, n = 6, Scheme 3A, Series I) by a Diels-Alder reaction of furans with vinyl sulfonates, all of them exhibited moderate-to-excellent binding affinity and nanomolar inhibition of HDAC (see below); moreover, during our work on OBHS-core ER ligands, we found that the size of the substituents on phenyl ring of the OBHS sulfonate moiety were important determinants of the binding affinity and selectivity of these compounds. Therefore, we wondered whether the chain length of HDACi unit was a critical variable in optimizing the positioning of ligand for ER or of zinc binding group (ZBG) for HDAC inhibition profiles. Thus, the success of the suberic acid conjugates prompted us to explore the biological effects of chain-length variation, and as a result, the pimelic (**30a-c**, linker length n = 5, Scheme 3A, Series I) and azelaic acid analogs (**32a-c**, linker length n = 7, Scheme 3A, Series I) were prepared, respectively. However, we found that the suberic acid conjugate had higher affinity than pimelic and azelaic acid analogs in favor of ERα; additionally, the suberic acid conjugate also had superior HDAC1 inhibition activity relative to the other two series (**30** and **32**). These results illustrate that the suberic acid unit (linker length n = 6) was essential for optimal biological activity. Therefore, when the HDACi unit was appended onto the phenyl ring of sulfonate moiety of OBHS (Scheme 3B, Series II), additional SAR investigations were also focused on the suberic acid derivative **33** rather than pimelic and azelaic acid analogs. However, we found **33** still showed poor binding affinity for both ERs (see below).

The Diels-Alder reaction of vinyl sulfonates with furans (**19a-c** or **29**) went very smoothly, and the yields of the products were generally good. Also, it is noteworthy that high stereoselectivity was observed in the reaction of furans with dienophiles; as we described previously,[30] the *exo* products predominated in the Diels-Alder reaction. It should be noted that the conjugates **30a-c**, **31a-c**, **32a-c**, and **33** were generated by the Diels-Alder reactions of vinyl sulfonates with the unsymmetrical furans, therefore, which were studied as a mixture of regioisomers that, despite our best efforts, could not be separated, the results were summarized in Table 1.

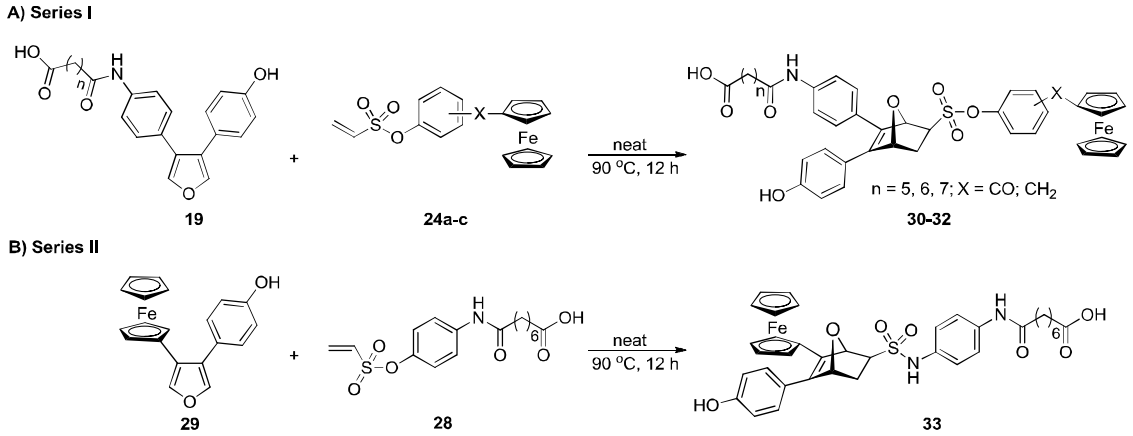

Scheme 3 Synthesis of FcOBHS-HDACi conjugates **30a-c**, **31a-c**, **32a-c**, and **33**

2.2. FcOBHS-HDACi Conjugates Exhibit Binding Affinity

The binding affinities of the FcOBHS-HDACi conjugates for both ERα and ERβ were determined by a competitive fluorometric receptor-binding assay and are summarized in Table 2;[35] the K_i values of the FcOBHS-HDACi conjugates are also summarized in Table 2. These affinities are presented as relative binding affinity (RBA) values, where estradiol has an affinity of 100%.

As a global observation, it is notable first that most of the conjugates (**30a-c**, **31b-c**, **32b-c**, **33**) show ER subtype selectivity for ERα of at least 1.5-fold in terms of RBA α/β ratio. Secondly, chain length has significant effects on the binding affinity of conjugates in Series I. We observed that the series of **31** that have a spacer length of n of 6 (n = 6) seemingly demonstrate a better ERα affinity than the other two series (**30**, n = 5 and **32**, n = 7). In fact, the suberic acid compound **31b** has the highest ERα affinity of all conjugates tested. The RBA values of this compound are 3.28 and 0.37 for ERα and ERβ, respectively, and it has an ERα/β selectivity as high as 8.86 (Table 2, entry 5). Compared to the parent OBHS-HDACi conjugate **11** (RBA values were 2.55 for ERα, 3.35 for ERβ, α/β was 0.76),[35] compound **31b** showed higher binding affinity for ERα and subtype selectivity. We are also aware of the position of the ferrocene on the phenyl group of sulfonate unit has significant effect on binding affinity of conjugates for ERα: when ferroceny-formyl group is moved from C3 to C4-position of the phenyl ring, results in an obvious increase in binding affinity for ERα (Table 2, **30a** vs **30b**; **31a** vs **31b**; **32a** vs **32b**). For example, **31b** shows a 5-fold affinity increase compared to **31a**. However, when the carbonyl group of ferroceny-formyl is reduced to a methylene group, a progressive decrease of binding affinity for ERα was observed (Table 2, **30b** vs **30c**; **31b** vs **31c**). These results illustrate that ferroceny-formyl at C4-position of the phenyl ring in sulfonate unit can enhance binding affinity for ERα; while the position of the ferroceny group has little effect on binding affinity for ERβ. For example, when ferroceny-formyl group is moved from C3 to C4-position of the phenyl sulfonate unit, pimelic acid conjugate **30b** shows a 1.9-fold increase over **30a (**Table 2, entries 1 vs 2); yet, suberic acid analogue **31b** results in a dramatically decreased binding affinity for ERβ (Table 2, entries 4 vs 5). In further attempts to increase the RBA, the suberic acid group was moved from the phenolic ring to the phenyl sulfonate moiety (compound **33**). This led, however, to a loss of binding affinity for both ERs, with an RBA value not exceeding 1 (entry 10). Compared to the parent OBHS-HDACi conjugate **12** (RBA values were 12.4 for ERα, 0.44 for ERβ, α/β was 28),[35] compound **33** showed about 31-fold weaker binding affinity for ERα and 18-fold weaker subtype selectivity.

Table 1 Diels-Alder Reaction of Furans **19**, **29** and Dienophiles **24a-c** and **28**

Entry	Furan	Dienophile	Conv.[a] (%)	Product Yield[b]
1	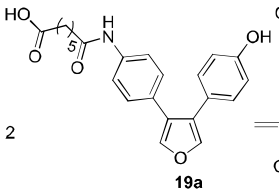 **19a**	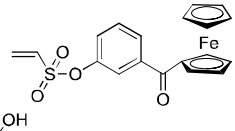 **24a**	99	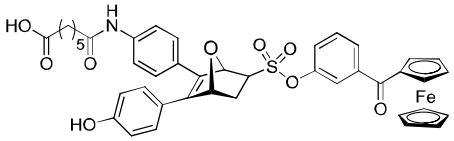 **30a** (94%)
2		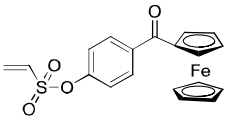 **24b**	97	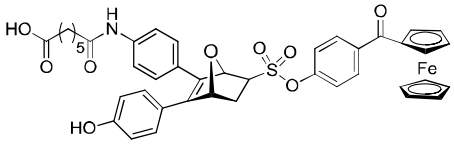 **30b** (95%)
3		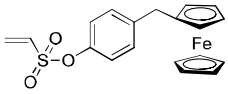 **24c**	96	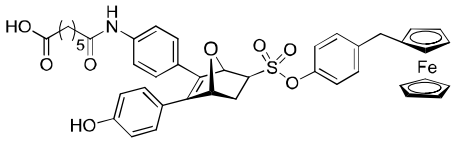 **30c** (93%)
4	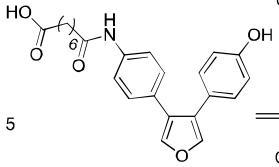 **19b**	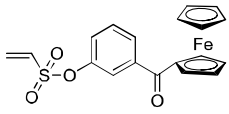 **24a**	98	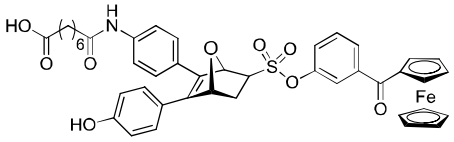 **31a** (95%)
5		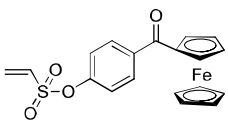 **24b**	97	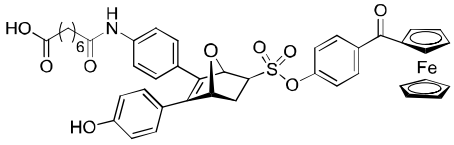 **31b** (94%)
6		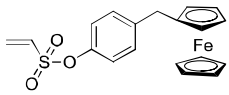 **24c**	98	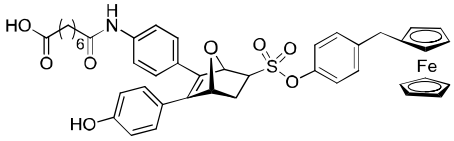 **31c** (95%)
7	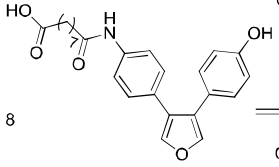 **19c**	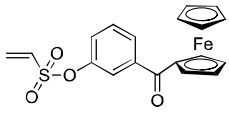 **24a**	96	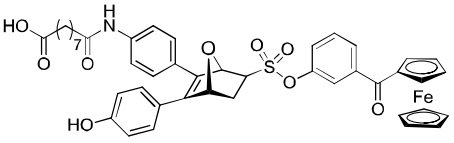 **32a** (94%)
8		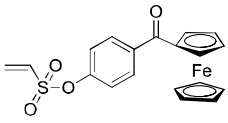 **24b**	99	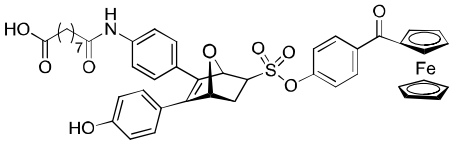 **32b** (97%)
9		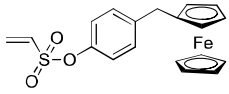 **24c**	98	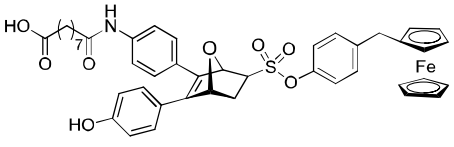 **32c** (95%)
10	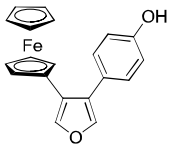 **29**	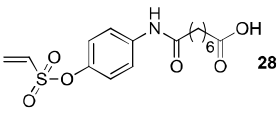 **28**	97	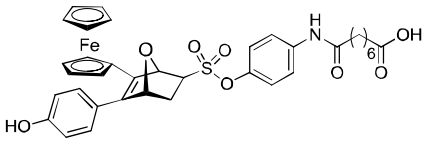 **33** (92%)

[a]The conversion was calculated accounting for the recovered furans **19a-c** or **29**. [b]Isolated yield by column chromatography purification based on furans **19a-c** or **29**.

Table 2 Relative Binding Affinity (RBA) of FcOBHS-HDACi Conjugates for ERα and ERβ[α]

Entry	Compound		RBA[a] (%) ERα	RBA[a] (%) ERβ	α/β ratio	K_i [b] (nM) ERα	K_i [b] (nM) ERβ	α/β ratio
1	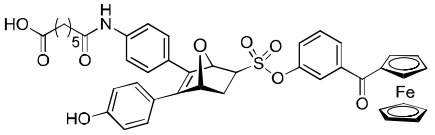	**30a**	0.21 ± 0.01	0.11 ± 0.01	1.91	1476.19	3090.91	2.09
2	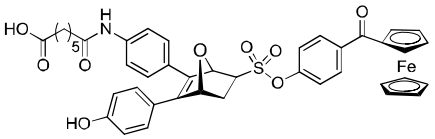	**30b**	1.71 ± 0.17	0.21 ± 0.04	8.14	181.29	1619.05	8.93
3	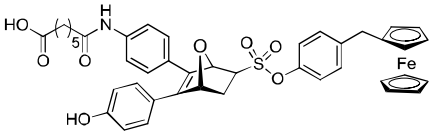	**30c**	0.43± 0.08	0.38 ± 0.02	1.12	720.93	894.74	1.24
4	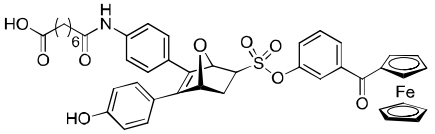	**31a**	0.64 ± 0.05	3.68 ± 0.33	0.17	484.37	92.39	0.19
5	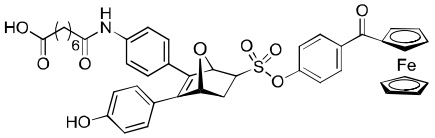	**31b**	3.28± 0.55	0.37 ± 0.01	8.86	94.51	918.92	9.72
6	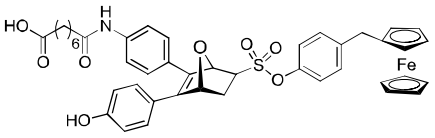	**31c**	1.64 ± 0.03	0.09 ± 0.01	18.22	189.02	3777.78	19.98
7	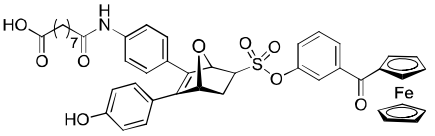	**32a**	0.23 ± 0.02	0.77 ± 0.01	0.29	1347.83	441.56	0.33
8	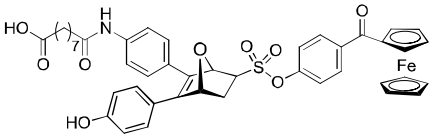	**32b**	0.38 ± 0.01	0.10 ± 0.01	3.80	815.79	3400.00	4.17
9	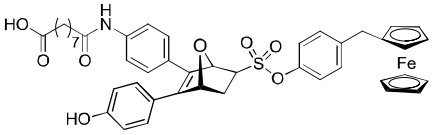	**32c**	1.97 ± 0.09	0.33 ± 0.02	5.97	157.36	1030.30	6.55
10	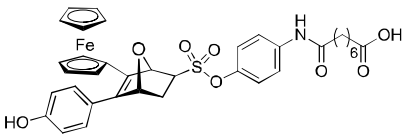	**33**	0.39 ± 0.05	0.26 ± 0.02	1.50	794.87	1307.69	1.65

[a]Relative Binding Affinity (RBA) values are determined by competitive flourometric binding assays and are expressed as $IC_{50}^{estradiol}$ / $IC_{50}^{compound}$ × 100 (RBA, estradiol = 100%). The values are reported as the mean ± standard deviation (mean ± SD) of three independent experiments. [b]K_i values of each conjugate for each receptor were obtained from the RBA values by the formula $K_i = (100/RBA) \times K_d$. The K_d value of estradiol is 3.1 nM for ERα and 3.4 nM for ERβ, respectively. For details, see Experimental Section.

2.3. Transcription Activation Assays

Various FcOBHS-HDACi conjugates were tested by an ER-responsive luciferase reporter gene assays for their ability to stimulate the transcriptional activities of ERα and ERβ compared to 17β-estradiol (E_2). Luciferase assays were conducted in HEK293T cells transfected with a widely used 3 × ERE-luciferase reporter. These results are summarized in Table 3.

As shown in this table, most of FcOBHS-HDACi conjugates examined are ERβ agonists, and compounds **30a-b (**Table 3, entries 1 vs 2**)** even exhibit full agonist activities. In fact, several compounds act as potent and nearly complete ERβ-selective agonists. In contrast, OBHS-HDACi conjugates display a wide range of activities at ERβ. These results demonstrate that very small changes to 7-oxabicyclic[2.2.1]hept-5-ene (OBHS)-core ligand structure can have drastic effects on the transcription activity.

In addition to this interesting activity, most of conjugates were found to act as ERα agonist. However, the effects of increasing chain length of HDACi unit were very evident. Compounds **30a-c**, which bearing the pimelic acid (n = 5) group on phenol ring, acting as ERα full agonist with nanomolar (nM) range EC_{50}s. In the case of compound **31**, however, replacing pimelic acid (n = 5) of compounds **30** with suberic acid (n = 6) have obvious effects on the transcriptional activity of the ERα. This suggests that ERα is more sensitive to OBHS-core ligand structure than ERβ, and that it can convert from an agonist to antagonist. For example, 3-ferroceny-formyl and ferroceny-benzyl compounds (**31a** and **31c)** are still the ERα agonists despite reduced efficacy, compared to their corresponding pimelic acid analogues (Table 3, entries 1 vs 4, 3 vs 6); whereas 4-ferroceny-formyl compound **31b** profiles as a full antagonist (entries 2 vs 5), which shows at least 3-fold more efficacious as ERα full antagonist than the parent OBHS-HDACi conjugate **11**. Interestingly, when the chain length of HDACi unit was changed from the pimelic acid (n = 5) to azelaic acid (n = 7), 3-ferroceny-formyl and ferroceny-benzyl compounds (**32a-b**) display agonist activity for ERα; especially, **31a** profiles as a superagonist on ERα, showing efficacy in ERα 1.1 times greater than that of estradiol (Table 3, entry 7); yet, the 4-ferroceny-formyl compound **32c** profiles as a full antagonist (Table 3, entry 9). However, compound **32c** with decreased binding affinity (Table 2, entries 5 vs 9), also shows decreased potency and efficacy as ERα antagonist, compare to suberic acid conjugate **31b** (Table 3, entries 5 vs 9). Here again, it is clear that the optimal chain length of HDACi unit is n = 6. Furthermore, introduction of the suberic acid to the phenyl sulfonate moiety (compound **33**, entry 10) also exhibits the typical ERα-selective full antagonist property, and shows about 2-fold more efficacious than the parent OBHS-HDACi conjugate **12**. Thus, the ability of compounds bearing OBHS scaffold to stimulate ERα activity does not correlate with their relative binding affinities for ERα.

Table 3 Effects of FcOBHS-HDACi Conjugates on the Transcriptional Activities of Estrogen Receptor α and β

		Agonist Mode[a]				Antagonist Mode[b]			
		ERα		ERβ		ERα		ERβ	
entry	cmpd	EC_{50} (μM)	Eff (% E_2)	EC_{50} (μM)	Eff (% E_2)	IC_{50} (μM)	Eff (% E_2)[c]	IC_{50} (μM)	Eff (% E_2)
1	**30a**	0.27	89 ± 2	2.32	92 ± 1	-	118 ± 3	-	105 ± 1
2	**30b**	0.99	76 ± 1	1.11	89 ± 5	-	123 ± 20	-	101 ± 4
3	**30c**	0.78	77 ± 8	1.57	36 ± 7	-	97 ± 16	-	96 ± 2
4	**31a**	1.70	46 ± 2	0.75	13 ± 2	-	95 ± 6	-	73 ± 1
5	**31b**	-	-4 ± 1	0.35	24 ± 3	1.10	4 ± 4	-	74 ± 3
6	**31c**	0.38	52 ± 6	0.36	17 ± 1	-	144 ± 8	-	89 ± 1
7	**32a**	1.17	112 ± 13	2.41	26 ± 3	-	118 ± 4	-	100 ± 6
8	**32b**	1.50	58 ± 11	-	-11 ± 1	-	106 ± 2	-	86 ± 7
9	**32c**	-	-10 ± 2	2.03	37 ± 4	2.38	27 ± 1	-	75 ± 11
10	**33**	-	-29 ± 1	-	-3 ± 1	0.57	14 ± 1	-	102 ± 2
11	**OBHS**	0.095	60 ± 2	-	0 ± 1	0.014	70 ± 12	0.581	-16 ± 2

[a]Luciferase activity was measured in HEK293T cells transfected with 3 × ERE-driven luciferase reporter and expression vectors

encoding ERα or ERβ and treated in triplicate with increasing doses (up to 10^{-5} M) of the compounds. EC_{50} and standard deviation (mean ± SD), shown as a percentage of 10^{-8} M 17β-estradiol (E_2), were determined. [b]IC_{50} and standard deviation (mean ± SD) were determined in the percentage of 10^{-8} M 17β-estradiol (E_2) on ERα or ERβ. [c]ERs have considerable basal activity in HEK293T cells; compounds with inverse agonist activity are given negative efficacy values. Omitted EC_{50} or IC_{50} values were too high to be determined accurately.

2.4. Structural Analysis of the Origin of Enhanced Antagonist Character of FcOBHS-HDACi Conjugates

The ability of the FcOBHS-HDACi conjugates to act as antagonists on ERα is not surprising because it is known that most of OBHS-core ligands profiles as antagonists. We are surprised, however, by the position of HDACi unit in dual-targeting FcOBHS-core ligands-HDACi conjugates. To understand why suberic acid compound is still able to exhibit full antagonist activity in different location of OBHS core, we have used molecular modeling to examine how some of these conjugates fit into the ligand binding pocket of ERα (Figure 4).

Crystal structure of the ERα LBD in complex with OBHS shows that one *p*-hydroxyphenyl group mimics the role of the A-ring phenol of E_2, engaging in strong hydrogen bonding with residue Glu353 of helix 3; while another *p*-hydroxyphenyl group forms a hydrogen bond with residue Thr347 in helix 3. The non-poplar phenyl sulfonate group in OBHS extends between helices 8 and 11, and which makes strong steric clashes with helix 11, displacing residue His524, which engages in hydrogen bonding interaction with E_2 (PDB ID: 1ERE). Displacement of Helix 11 indirectly modulates the conformation of the critical helix 12 and transcriptional activity (Figure 4A), a mechanism we have termed "passive antagonism".

Consistent with this model, OBHS-HDACi conjugate (Figure 4B) can similarly form a hydrogen bond between the *p*-hydroxyphenyl group and helix 3 residue Glu353, and the sulfonate side chain makes clash with helix 11; interestingly, suberic acid side chain mimics the binding orientation of 4-hydroxytamoxifen, however, which does not directly interact with any of helix 12 residues. Instead, the suberic acid side chain forms hydrogen bond contacts with helix 3 (Ser 341, Leu 345, and Leu 346) which can provide subtle shifts in helix 3 that destabilize helix 12, thus giving OBHS-HDACi potent ERα antagonist activity. Similar to OBHS-HDACi conjugate **11**, the *p*-hydroxyphenyl group of FcOBHS-HDACi conjugate **31b** also engages in the crucial hydrogen bonding with Glu353, which simulates the interaction of the A-ring of steroidal estrogens in ERα complexes, but suberic acid side chain can directly interfere with helix 12 (Figure 4C), which is consistent with the action model of 4-hydroxytamoxifen (Figure 4D). Thus, FcOBHS-HDACi conjugate represents a novel mechanism to generate a full ERα antagonist which is distinct from that of OBHS-core ligands.

2.5. Conjugates Exhibit Potent HDAC Inhibition Activity

We tested all of FcOBHS-HDACi conjugates for HDAC inhibition activity against HDAC1 and HDAC6, respectively (Table 4). Although overexpression of HDAC1, HDAC6 and HDAC8 have been linked to breast cancer,[46] HDAC1 and HDAC6 have been found to be more critical.[26, 29] As shown by the data in Table 4, the HDAC inhibition activity was very much dependent on the length of the acid chain of FcOBHS-HDACi conjugates. In general, Series I suberic acid conjugates (**31a-c**, linker length n = 6) strongly inhibit HDAC1 (with nanomolar range IC_{50}s), are demonstrated to be highly selective for HDAC1, having modest or no active against HDAC6; actually, suberic acid conjugate **31b** shows the most potent anti-HDAC1 (IC_{50} = 197 nM) activity; yet, the parent OBHS-HDACi conjugate **11** is essentially inactive for either of the HDACs.[35] However, either shorter (**30a-c**, n = 5) or longer chain lengths (**32a-c**, n = 7) result in reduced potency, specifically, the seven methylene-linked compounds **31b-c** are inactive against HDAC1; additionally, both pimelic acid (n = 5) and azelaic acid (n = 7) conjugates are not selective for HDACs. Interestingly, when suberic acid group is appended onto the phenyl ring of sulfonate moiety, compound **33** also displayed good inhibition preference for HDACs with the nanomolar range (Table 4, entry 10), which is 56-fold more potent than the parent OBHS-HDACi conjugate **12** in HDAC6 inhibition (with IC_{50} value of 8.34 μM for HDAC6). [35]

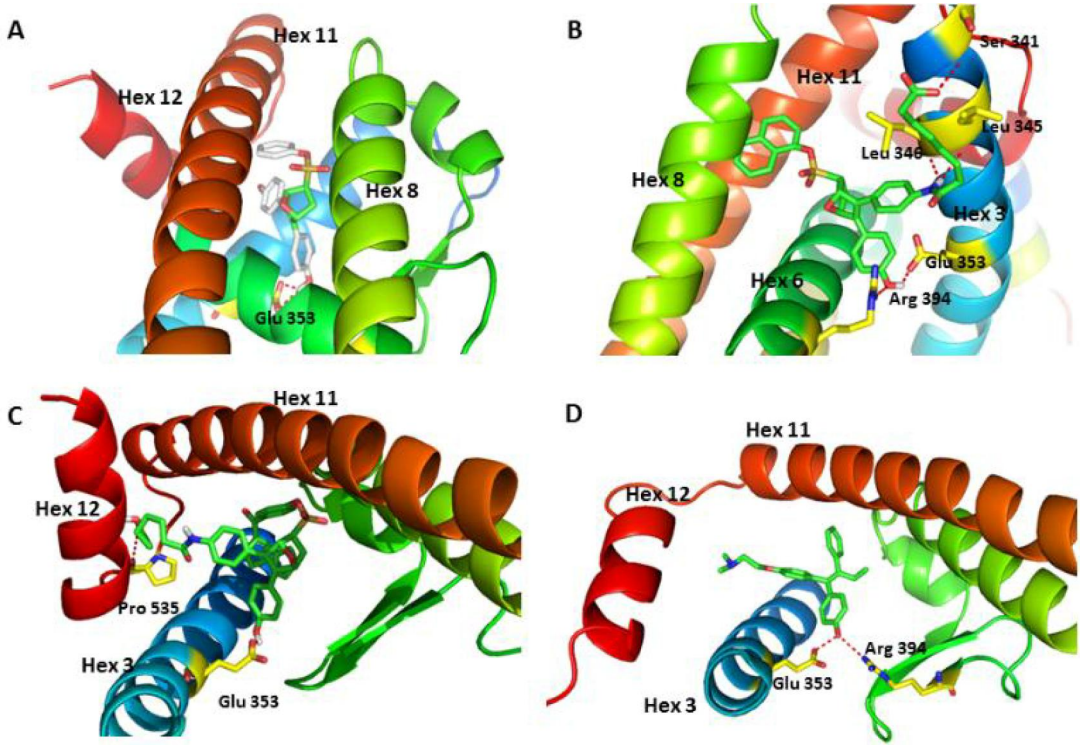

Figure 4 Model of FcOBHS-HDACi conjugates bound to ERα and comparisons with OBHS, OBHS-HDACi conjugate and 4-hydroxytamoxifen. (A) Crystal structure of the ERα LBD in complex with oxabicyclic heptane sulfonate (OBHS) bound ERα.[30] OBHS H-bonds to the conserved Glu 353 on helix 3. The phenyl sulfonate binds between helices 8 and 11. (B) Computer-developed model of OBHS-HDAC conjugate **11** bound to ERα with the conserved H-bonding to Arg 394, Ser 341, Leu 345, Leu 346 and Glu 353, and the sulfonate moiety extending between helices 8 and 11.[35] (C) Computer-developed model of **31b** forms hydrogen bonds with Glu 353, and the suberic acid side chain makes a distinct hydrogen bonding interaction with H12, which directly displaces helix 12; moreover, the ferrocenyl group clashes with helix 3. (D) Crystal structure of the ERα LBD in complex with 4-hydroxytamoxifen (4OHT, PDB: 3ERT). 4-OHT forms hydrogen bonds with Glu 353 and Arg 394, the side chain displaces helix 12.[45]

2.6. Whole Cell Antiproliferative Activity

To evaluate their anticancer activity, all dual-acting conjugates were screened against MCF-7 (hormone-dependent breast cancer cells), MDA-MB-231 (hormone-independent breast cancer cells), DU-145 (hormone-refractory, metastatic prostate cancer cells), as well as one control cell line, healthy kindney epithelial cells (VERO), and the results are summarized in Table 5.

A closer analysis of the cell growth inhibition data in Table 5 reveals that introduction of ferrocenyl group on phenyl ring of sulfonate unit of OBHS-HDACi conjugates shows significant antiproliferative effect on MDA-MB-231 breast cancer cells (Table 5, entries 2 vs 6; 2 vs 7; 2 vs 8), unlike the parent OBHS-HDACi conjugates **11** and **12**, which show a weaker activity (IC_{50} > 50.0 μM). Specifically, **31b** stands out among these FcOBHS-HDACi conjugates because it shows the best antiproliferative activity, which is about 1.2-fold more potent than 4OHT (Table 5, entries 7 vs 14), against MDA-MB-231 cells; moreover, they retain great activity of their parent compounds against MCF-7 cells. This observation indicates that antiproliferative activity of these FcOBHS-HDACi conjugates against MDA-MB-231 cells derives mainly from ferrocenyl group. While antiproliferative activities of these dual-acting conjugates **30-33** are very dependent on the linker length, and also closely matched their anti-HDAC activities. We noticed that compounds **30a-c**, with the shortest linker of five methylenes, also were effective in inhibiting the MDA-MB-231 cells, but they showed weaker inhibition for MCF-7 cells than the corresponding six-methylene compound (Table 5, entries 3 vs 6; 4 vs 7). Surprisingly, compounds **32b-c** with a spacer length of seven methylenes show the least antiproliferative activities against MDA-MB-231 and DU 145 cells; actually, they are essentially inactive, an observation which agrees with its poor

Table 4 IC_{50} values of conjugates for inhibition of HDAC1 and HDAC6[a]

Entry	Compd		HDAC1 [μM]	HDAC6 [μM]
1	**30a**	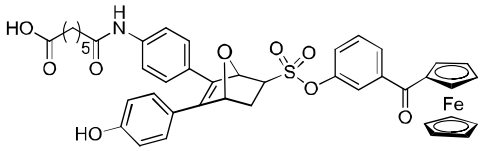	0.353	0.181
2	**30b**	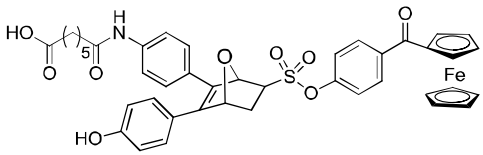	1.40	1.07
3	**30c**	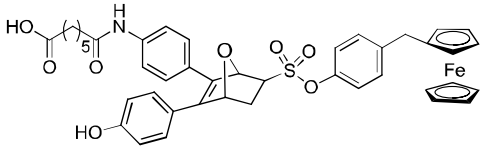	1.17	ND[b]
4	**31a**	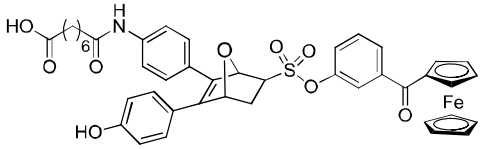	0.211	0.299
5	**31b**	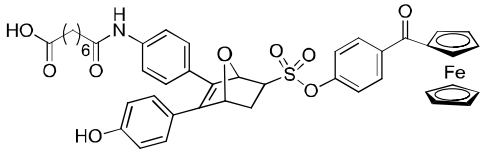	0.197	0.436
6	**31c**	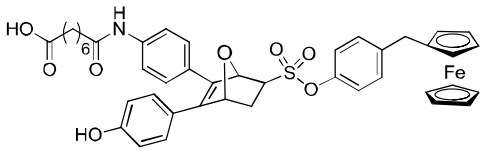	0.660	ND
7	**32a**	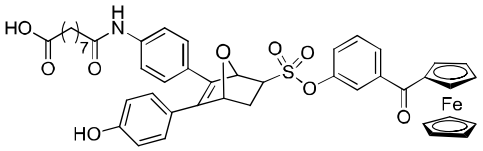	0.224	0.131
8	**32b**	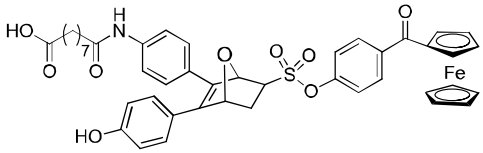	ND	4.51
9	**32c**	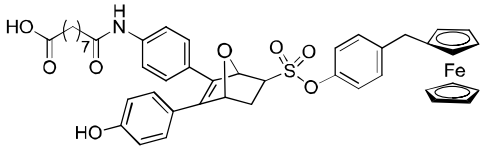	ND	ND
10	**33**	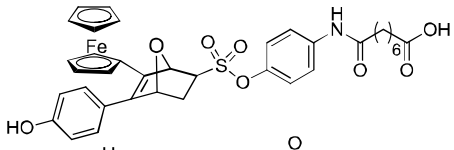	0.546	0.147
11	**Vorinostat (SAHA)**	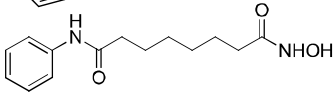	0.0474	0.0297

[a]Values are the means of a minimum of three experiments. [b]ND = inhibition not detectable.

HDAC inhibition profile. However, when suberic acid group is appended onto the phenyl ring of sulfonate moiety, compound **33** still possesses potent antiproliferative activities both ER(+) and ER(-) breast cancer cells (Table 5, entry 12). These results suggest that inhibition of HDAC also can enhance potency against MDA-MB-231 cells.

Another interesting aspect of antiproliferative activity is that most conjugates showed significant antiproliferative effects on DU 145 cells, which only express ERβ. This result suggests that these FcOBHS-HDACi conjugates may have potential benefit against ERβ dependent cancers.

Additionally, all FcOBHS-HDACi conjugates are nontoxic to healthy VERO cells, while SAHA and 4OHT showed considerable toxicity. Comparing the activity of conjugates (**30c**, **31a-c**, and **33**), which showed significant antiproliferative effects on both ER(+) and ER(-) breast cancer cells, with control drugs SAHA and tamoxifen on VERO, 4OHT had the smallest *in vitro* therapeutic index (IVTI), while our conjugates show greater IVTIs (Table 6).

Table 5 Whole cell antiproliferative activity (IC_{50}, μM)[a]

Entry	Cmpd	MCF-7	MDA-MB-231	DU-145	VERO
1	**OBHS**	20.9 ± 1.00	>50[b]	>50	>50
2	**12**	19.1 ± 1.09	>50	34.8 ± 2.91	>50
3	**30a**	49.1 ± 0.85	18.4 ± 0.12	17.0 ± 0.21	>50
4	**30b**	41.4 ± 1.66	18.9 ± 2.54	30.3 ± 1.21	>50
5	**30c**	22.8 ± 2.04	21.1 ± 0.22	35.6 ± 1.05	>50
6	**31a**	26.4 ± 0.97	18.8 ± 0.62	25.5 ± 0.80	>50
7	**31b**	14.8 ± 0.35	15.5 ± 0.49	25.3 ± 0.30	>50
8	**31c**	24.5 ± 0.56	20.1 ± 0.19	34.2 ± 1.66	>50
9	**32a**	>50	17.1 ± 1.12	25.3 ± 0.12	>50
10	**32b**	>50	>50	>50	>50
11	**32c**	44.1 ± 0.59	>50	>50	>50
12	**33**	15.6 ± 0.34	17.1 ± 0.33	21.2 ± 2.01	>50
13	**SAHA**	2.5 ± 0.33	1.8 ± 0.07	1.2 ± 0.07	4.1 ± 0.19
14	**4OHT**	15.6 ± 1.77	18.8 ± 0.57	15.3 ± 4.42	15.1 ± 5.21

[a]IC_{50} values are an average of at least three independent experiments ± standard deviation (mean ± SD). [b]IC_{50} not determinable up to highest concentrations tested.

Table 6 *In vitro* therapeutic index (IVTI) of FcOBHS-HDACi conjugates **30c**, **31a-c**, and **33**

Entry	Compound	*IVTI*[a]	*IVTI*[b]
1	**30c**	> 2.19	> 2.36
2	**31a**	> 1.89	> 2.65
3	**31b**	> 3.37	> 3.22
4	**31c**	> 2.04	> 2.48
5	**33**	> 3.20	> 2.92
6	**SAHA**	1.64	2.27
7	**4OHT**	0.97	0.80

[a]IVTI = IC_{50}(VERO) / IC_{50}(MCF-7); [b]IVTI = IC_{50}(VERO) / IC_{50}(MDA-MB-231).

3. Conclusions

Breast cancer is a multifactorial disease involving multiple cross-talks between signaling networks. The estrogen receptor (ER) plays a predominant role in breast cancer growth, and which is regarded as important pharmaceutical target for the treatment of breast cancer.[47] Similarly, HDACs inhibitors exert antitumor effects by altering gene transcription and disrupting mitosis. To further improve the biological response of OBHS-HDACi conjugates, particularly against ER(-) breast cancer cells, we have created dual-acting FcOBHS-HDACi conjugates. A subset of these conjugates exhibited good binding affinity and excellent ERα antagonist activity. Careful analysis of their ER binding affinity output showed that they are largely ERα-selective. Docking analyses of FcOBHS-HDACi conjugate reveals a novel mechanism of antagonism via suberic acid group substitutions on the bicyclic core that directly obstructs helix 12, unlike OBHS-HDACi conjugate, which indirectly modulates the critical switch helix 12, by interactions with helix 3; moreover, these conjugates strongly inhibit HDAC1 and HDAC6. Excitingly, they show anticancer activity that is selectively more potent against MDA-MB-231 compared to MCF-7 or DU 145, and all conjugates are nontoxic to health VERO cells. While linker length of HDACi unit is a critical factor for activity, and conjugates with a shorter rather than longer chain length tend to be more active, especially those with suberic acid derivatives. Actually, the most promising compound of this study is suberic acid derivative **31b**, which has the highest binding affinity for ERα and exhibits ERα full antagonist activity, which also show the most potent anti-HDAC1 (IC_{50} = 197 nM) activity and against both ER(+) and ER(-) breast cancer cells. In summary, we have demonstrated that conjugation of ferrocenyl group to anticancer agents is a viable strategy to improve the biological response of the latter.

4. Experimental Section

4.1. Chemistry

4.1.1. General

Unless otherwise noted, starting materials were purchased from commercial suppliers and were used without further purification. Tetrahydrofuran (THF) was dried over Na and distilled prior to use. Dichloromethane and triethylamine were dried over CaH_2 and distilled prior to use. Glassware was oven-dried, assembled while hot, and cooled under an inert atmosphere. All reactions were performed under an argon atmosphere unless otherwise specified. Reaction progress was monitored using analytical thin-layer chromatography (TLC). Visualization was achieved by UV light (254 nm). ^{1}H NMR and ^{13}C NMR spectra were measured on a Bruker Biospin AV400 (400 MHz) instrument. Chemical shifts are reported in parts per million (ppm) and are referenced to either tetramethylsilane or the solvent.

4.1.2. General procedure for Diels-Alder reaction (30a-c, 31a-c, 32a-c, and 33). Furan **19** or **29** (0.7 mmol) and dienophile (**24a-c** or **28**, 0.84 mmol) were in a round flask, and the reaction mixture was stirred at 90 °C for 12 h. The crude product was purified by silica gel column chromatography (Dichloromethane-MeOH, 60 : 1~30 : 1).

4.1.2.1. 7-((4-(3-(4-Hydroxyphenyl)-6-((3-ferrocenylformyl) phenoxysulfonyl)-7-oxabicyclo[2.2.1]hept-2-en-2-yl)phenyl) amino)-7-oxo-heptanoic Acid (30a). Red soild, 95% yield, mp 154-156 °C; ^{1}H NMR (400 MHz, Acetone-d_6) δ 9.34 (s, 1H), 8.01 (s, 1H), 7.86 (d, J = 7.6 Hz, 1H), 7.65 (t, J = 7.2 Hz, 2H), 7.55 (m, 1H), 7.47 (t, J = 8.0 Hz, 1H), 7.35 (t, J = 8.8 Hz, 2H), 7.27 (t, J = 8.8 Hz, 2H), 6.86 (t, J = 8.4 Hz, 2H), 5.78 (s, 1H), 5.51 (s, 1H), 4.89 (s, 2H), 4.66 (s, 2H), 4.24 (s, 5H), 3.98 (m, 1H), 2.52 (m, 1H), 2.40 (m, 3H), 2.29 (t, J = 6.8 Hz, 2H), 1.71 (t, J = 6.8 Hz, 2H), 1.62 (t, J = 7.2 Hz, 2H), 1.41 (m, 2H). ^{13}C NMR (100 MHz, Acetone-d_6) δ 197.45, 175.10, 172.50, 158.66, 158.59, 149.98, 143.61, 142.30, 141.97, 140.15, 139.23, 137.53, 131.12, 130.19, 129.80, 128.98, 128.59, 127.58, 125.99. 124.61, 122.98, 120.40, 116.56, 85.19, 83.82, 78.71, 73.91, 72.16, 71.17, 62.11, 37.64, 34.18, 31.68, 31.47, 26.02, 25.42; HRMS (ESI) calcd for $C_{42}H_{38}{}^{54}FeNO_9S$ [M - H]$^-$, 786.6624; found 786.6621.

4.1.2.2. 7-((4-(3-(4-Hydroxyphenyl)-6-((4-ferrocenylformyl) phenoxysulfonyl)-7-oxabicyclo[2.2.1]hept-2-en-2-yl)phenyl) amino)-7-oxo-heptanoic Acid (30b). Red soild, 93% yield, mp 158-161 °C; ^{1}H NMR (400 MHz, Acetone-d_6) δ 9.31 (s, 1H), 8.00 (d, J = 8.0 Hz, 2H), 7. 67 (d, J = 8.4 Hz, 1H), 7.63 (d, J = 8.4 Hz, 1H), 7.43 (t, J = 8.0 Hz, 2H), 7.36 (d, J = 8.0 Hz, 1H), 7.32 (t, J = 7.6 Hz, 2H), 7.26 (d, J = 8.0 Hz, 1H), 6.88 (d, J = 8.0 Hz, 1H), 6.83 (d, J = 8.0 Hz, 1H), 5.76 (s, 1H), 5.50 (s, 1H), 4.84 (s, 2H), 4.66 (s, 2H), 4.23 (s, 5H), 3.95 (m, 1H), 2.51 (m, 1H), 2.39 (m, 3H), 2.32 (t, J = 7.2 Hz, 2H), 1.70 (m, 2H), 1.62 (t, J = 7.2 Hz, 2H), 1.41 (m, 2H). ^{13}C NMR (100 MHz, Acetone-d_6) δ 197.40, 174.90, 172.30, 158.70, 158.56, 152.60, 143.55, 142.00, 140.35, 140.21, 139.32, 137.54, 130.92, 130.34, 129.78, 129.12, 128.47, 127.94, 123.87. 123.03, 120.29, 120.10, 116.71, 116.51, 85.28, 83.73, 78.93, 73.66, 72.17, 71.07, 61.81, 37.61, 34.12, 31.57, 31.36, 25.98, 25.41; HRMS (ESI) calcd for

$C_{42}H_{38}{}^{54}FeNO_9S$ [M - H]$^-$, 786.6624; found 786.6621.

4.1.2.3. 7-((4-(3-(4-Hydroxyphenyl)-6-((4-ferrocenyl benzyl) phenoxysulfonyl)-7-oxabicyclo[2.2.1]hept-2-en-2-yl)phenyl) amino)-7-oxo-heptanoic Acid (30c). Red soild, 94% yield, mp 147-150 °C; ^{1}H NMR (400 MHz, Acetone-d_6) δ 9.14 (s, 1H), 7.53 (t, J = 8.8 Hz, 2H), 7. 17 (d, J = 7.6 Hz, 1H), 7.15 (d, J = 7.2 Hz, 1H), 7.11 (d, J = 7.6 Hz, 1H), 7.09 (d, J = 7.6 Hz, 1H), 7.05 (d, J = 8.8 Hz, 2H), 7.00 (d, J = 7.2 Hz, 1H), 6.99 (d, J = 7.2 Hz, 1H), 6.71 (d, J = 8.8 Hz, 1H), 6.68 (d, J = 8.8 Hz, 1H), 5.53 (s, 1H), 5.31 (t, J = 3.2 Hz, 1H), 3.97 (s, 7H), 3.92 (s, 2H), 3.64 (m, 1H), 3.60 (m, 2H), 2.27 (m, 3H), 2.17 (m, 3H), 1.58 (t, J = 7.6 Hz, 2H), 1.46 (t, J = 7.6 Hz, 2H), 1.30 (m, 2H). ^{13}C NMR (100 MHz, Acetone-d_6) δ 174.83, 172.18, 158.56, 158.42, 148.63, 142.13, 141.90, 140.21, 140.09, 139.24, 137.59, 130.60, 130.29, 129.11, 128.46, 127.95, 124.71, 123.90, 122.84, 120.23, 116.40, 88.54, 85.22, 83.64, 69.43, 69.36, 68.39, 61.21, 37.55, 35.90, 34.08, 31.51, 31.31, 25.98, 25.39; HRMS (ESI) calcd for $C_{42}H_{40}{}^{54}FeNO_8S$ [M - H]$^-$, 772.1824; found 772.1820.

4.1.2.4. 8-((4-(3-(4-Hydroxyphenyl)-6-((3-ferrocenylformyl) phenoxysulfonyl)-7-oxabicyclo[2.2.1]hept-2-en-2-yl)phenyl) amino)-8-oxo-octanoic Acid (31a). Red soild, 93% yield, mp 162-164 °C; ^{1}H NMR (400 MHz, Acetone-d_6) δ 9.27 (s, 1H), 8.00 (s, 1H), 7.84 (d, J = 7.6 Hz, 1H), 7.65 (t, J = 7.2 Hz, 2H), 7.55 (m, 1H), 7.48 (t, J = 8.0 Hz, 1H), 7.34 (t, J = 8.0 Hz, 2H), 7.24 (t, J = 8.4 Hz, 2H), 6.83 (t, J = 8.4 Hz, 2H), 5.76 (s, 1H), 5.50 (s, 1H), 4.86 (s, 2H), 4.66 (s, 2H), 4.25 (s, 5H), 3.93 (m, 1H), 2.52 (m, 1H), 2.38 (t, J = 7.2 Hz, 3H), 2.29 (t, J = 7.2 Hz, 2H), 1.69 (t, J = 6.8 Hz, 2H), 1.61 (t, J = 6.4 Hz, 2H), 1.37 (m, 4H). ^{13}C NMR (100 MHz, Acetone-d_6) δ 197.30, 175.06, 172.44, 158.62, 158.56, 150.01, 143.57, 142.32, 142.02, 140.26, 139.20, 137.57, 131.08, 129.77, 128.57, 127.53, 125.95, 124.65, 123.94, 123.01, 122.95, 120.32, 85.19, 83.77, 78.74, 73.83, 72.08, 71.07, 61.94, 55.92, 37.74, 34.21, 31.45, 26.15, 25.54, 29.63; HRMS (ESI) calcd for $C_{43}H_{40}{}^{54}FeNO_9S$ [M - H]$^-$, 800.1829; found 800.1825.

4.1.2.5. 8-((4-(3-(4-Hydroxyphenyl)-6-((4-ferrocenylformyl) phenoxysulfonyl)-7-oxabicyclo[2.2.1]hept-2-en-2-yl)phenyl) amino)-8-oxo-octanoic Acid (31b). Red soild, 96% yield, mp 160-163 °C; ^{1}H NMR (400 MHz, Acetone-d_6) δ 9.34 (s, 1H), 7.97 (d, J = 8.4 Hz, 2H), 7.64 (m, 2H), 7.41 (t, J = 7.6 Hz, 2H), 7.34 (d, J = 8.0 Hz, 1H), 7.32 (t, J = 8.0 Hz, 2H), 7.24 (d, J = 8.0 Hz, 1H), 6.88 (d, J = 8.0 Hz, 1H), 6.81 (d, J = 8.0 Hz, 1H), 5.76 (s, 1H), 5.50 (s, 1H), 4.84 (s, 2H), 4.65 (s, 2H), 4.23 (s, 5H), 3.96 (m, 1H), 2.50 (m, 1H), 2.39 (m, 2H), 2.31 (m, 2H), 1.68 (m, 2H), 1.61 (t, J = 6.0 Hz, 2H), 1.36 (m, 4H). ^{13}C NMR (100 MHz, Acetone-d_6) δ 197.58, 175.19, 172.59, 158.73, 158.59, 152.59, 141.97, 139.25, 137.50, 130.95, 130.35, 129.72, 129.12, 128.51, 128.00, 124.64, 123.84, 123.09, 123.06, 120.39, 120.20, 116.75, 116.56, 85.22, 83.70, 78.88, 73.74, 72.21, 71.11, 61.84, 37.77, 34.28, 31.59, 31.38, 29.68, 26.16, 25.66; HRMS (ESI) calcd for $C_{43}H_{40}{}^{54}FeNO_9S$ [M - H]$^-$, 800.1829; found 800.1825.

4.1.2.6. 8-((4-(3-(4-Hydroxyphenyl)-6-((4-ferrocenyl benzyl) phenoxysulfonyl)-7-oxabicyclo[2.2.1]hept-2-en-2-yl)phenyl) amino)-8-oxo-octanoic Acid (31c). Red soild, 92% yield, mp 153-155 °C; ^{1}H NMR (400 MHz, Acetone-d_6) δ 9.31 (s, 1H), 7.67 (t, J = 8.8 Hz, 2H), 7.30 (m, 2H), 7.23 (t, J = 7.6 Hz, 2H), 7.18 (d, J = 8.4 Hz, 2H), 7.14 (d, J = 7.6 Hz, 1H), 7.12 (d, J = 7.6 Hz, 1H), 6.85 (d, J = 8.4 Hz, 1H), 6.82 (d, J = 8.4 Hz, 1H), 5.67 (s, 1H), 5.44 (s, 1H), 4.15 (s, 7H), 4.10 (s, 2H), 3.76 (m, 1H), 3.65 (s, 2H), 2.40 (m, 3H), 2.29 (m, 3H), 1.70 (t, J = 6.0 Hz, 2H), 1.59 (m, 2H), 1.37 (m, 4H). ^{13}C NMR (100 MHz, Acetone-d_6) δ 175.13, 172.50, 158.66, 158.52, 148.61, 142.11, 139.26, 137.56, 130.63, 130.61, 130.30, 129.66, 129.11, 128.47, 124.69, 123.89, 122.90, 122.80, 120.39, 120.15, 116.72, 116.51, 85.25, 83.64, 69.56, 69.47, 68.51, 61.25, 55.04, 37.77, 35.90, 31.52, 31.32, 26.18, 25.63; HRMS (ESI) calcd for $C_{43}H_{42}{}^{54}FeNO_8S$ [M - H]$^-$, 786.1976; found 786.1951.

4.1.2.7. 9-((4-(3-(4-Hydroxyphenyl)-6-((3-ferrocenylformyl) phenoxysulfonyl)-7-oxabicyclo[2.2.1]hept-2-en-2-yl)phenyl) amino)-9-oxo-nonanoic Acid (32a). Red soild, 93% yield, mp 165-167 °C; ^{1}H NMR (400 MHz, Acetone-d_6) δ 9.30 (s, 1H), 8.00 (s, 1H), 7.86 (d, J = 7.6 Hz, 1H), 7.65 (t, J = 7.6 Hz, 2H), 7.56 (m, 2H), 7.50 (t, J = 8.0 Hz, 1H), 7.35 (t, J = 8.8 Hz, 2H), 7.30 (d, J = 7.2 Hz, 1H), 7.27 (t, J = 8.8 Hz, 2H), 6.85 (t, J = 8.8 Hz, 2H), 5.77 (s, 1H), 5.51 (t, J = 3.6 Hz, 1H), 4.86 (s, 2H), 4.66 (s, 2H), 4.25 (s, 5H), 3.99 (m, 1H), 2.52 (m, 1H), 2.39 (m, 3H), 2.29 (m, 2H), 1.68 (t, J = 7.2 Hz, 3H), 1.58 (t, J = 6.8 Hz, 3H), 1.34 (m, 4H). ^{13}C NMR (100 MHz, Acetone-d_6) δ 197.38, 175.10, 172.54, 158.61, 158.55, 149.99, 143.59, 142.30, 141.99, 142.30, 141.99, 140.24, 139.21, 137.56, 131.10, 130.19, 129.80, 128.97, 128.59, 127.56, 125.97, 124.65, 122.98, 120.37, 116.54, 85.20, 83.81, 78.73, 73.87, 72.11, 71.15, 61.97, 37.81, 37.78, 34.27, 31.68, 31.47, 29.73, 26.27, 25.65; HRMS (ESI) calcd for $C_{44}H_{42}{}^{54}FeNO_9S$ [M - H]$^-$, 814.1930; found 814.1928.

4.1.2.8. 9-((4-(3-(4-Hydroxyphenyl)-6-((4-ferrocenylformyl) phenoxysulfonyl)-7-oxabicyclo[2.2.1]hept-2-en-2-yl)phenyl)

amino)-9-oxo-nonanoic Acid (32b). Red soild, 96% yield, mp 162-165 °C; ^{1}H NMR (400 MHz, Acetone-d_6) δ 9.29 (s, 1H), 8.00 (d, J = 8.4 Hz, 2H), 7.69 (d, J = 8.4 Hz, 1H), 7.64 (d, J = 8.8 Hz, 1H), 7.43 (t, J = 8.4 Hz, 2H), 7.35 (d, J = 8.4 Hz, 2H), 7.32 (t, J = 8.4 Hz, 1H), 7.26 (d, J = 8.4 Hz, 1H), 6.88 (d, J = 8.0 Hz, 1H), 6.83 (d, J = 8.4 Hz, 1H), 5.77 (s, 1H), 5.50 (s, 1H), 4.84 (s, 2H), 4.65 (s, 2H), 4.23 (s, 5H), 3.95 (m, 1H), 2.51 (m, 1H), 2.39 (m, 3H), 2.31 (t, J = 7.6 Hz, 2H), 1.68 (m, 3H), 1.59 (t, J = 6.4 Hz, 3H), 1.33 (m, 4H). ^{13}C NMR (100 MHz, Acetone-d_6) δ 197.50, 175.11, 172.56, 158.67, 158.53, 152.60, 143.56, 141.63, 139.30, 137.53, 130.94, 130.36, 129.72, 129.13, 128.51, 124.68, 123.89, 123.05, 116.72, 116.53, 85.23, 83.75, 78.91, 73.70, 72.20, 71.09, 62.03, 37.81, 34.27, 31.58, 31.37, 29.84, 29.73, 26.26, 25.65; HRMS (ESI) calcd for $C_{44}H_{42}{}^{54}FeNO_9S$ [M - H]$^-$, 814.1930; found 814.1928.

4.1.2.9. 9-((4-(3-(4-Hydroxyphenyl)-6-((4-ferrocenyl benzyl) phenoxysulfonyl)-7-oxabicyclo[2.2.1]hept-2-en-2-yl)phenyl) amino)-9-oxo-nonanoic Acid (32c). Red soild, 95% yield, mp 155-158 °C; ^{1}H NMR (400 MHz, Acetone-d_6) δ 9.25 (s, 1H), 7.65 (t, J = 8.8 Hz, 2H), 7.30 (d, J = 8.0 Hz, 1H), 7.28 (d, J = 7.6 Hz, 1H), 7.25 (t, J = 8.4 Hz, 2H), 7.18 (t, J = 8.4 Hz, 2H), 7.14 (d, J = 8.4 Hz, 2H), 6.85 (d, J = 8.8 Hz, 1H), 6.79 (d, J = 8.4 Hz, 1H), 5.67 (s, 1H), 5.45 (t, J = 3.6 Hz, 1H), 4.11 (s, 7H), 4.06 (s, 2H), 3.77 (m, 1H), 3.69 (m, 2H), 2.43 (m, 3H), 2.31 (t, J = 7.6 Hz, 3H), 1.68 (t, J = 6.4 Hz, 3H), 1.59 (m, 3H), 1.34 (m, 4H). ^{13}C NMR (100 MHz, Acetone-d_6) δ 174.95, 172.34, 158.54, 158.41, 148.58, 143.42, 142.24, 142.13, 141.90, 139.24, 137.59, 130.60, 130.30, 129.66, 129.12, 128.47, 124.73, 123.92, 122.79, 120.24, 116.41, 88.56, 85.22, 83.60, 69.44, 69.37, 68.40, 61.32, 37.74, 35.91, 34.21, 31.52, 31.30, 29.83, 26.26, 25.64; HRMS (ESI) calcd for $C_{44}H_{44}{}^{54}FeNO_8S$ [M - H]$^-$, 800.2138; found 800.2137.

4.1.2.10. 8-(4-(((5-(4-Hydroxyphenyl)-6-ferroceny-7-oxabicy-clo[2.2.1]hept-5-en-2-yl)sulfonyl)oxy)phenylamino)-8- oxooc-tanoic Acid (33). Red soild, 93% yield, mp 162-164 °C; ^{1}H NMR (400 MHz, Acetone-d_6) δ 9.32 (s, 1H, -NH_2), 8.37 (s, 1H, -OH), 7.74 (d, J = 8.8 Hz, 1H), 7.36 (d, J = 8.4 Hz, 2H), 7.35 (d, J = 8.4 Hz, 2H), 6.89 (d, J = 8.8 Hz, 2H), 5.56 (s, 1H), 5.39 (s, 1H), 4.35 (s, 2H), 4.28 (s, 2H), 4.18 (s, 5H), 3.82 (m, 1H), 2.42 (m, 1H), 2.36 (t, J = 6.8 Hz, 2H), 2.28 (m, 2H), 2.22 (m, 1H), 1.69 (t, J = 6.0 Hz, 2H), 1.59 (t, J = 6.8 Hz, 2H), 1.35 (m, 2H). ^{13}C NMR (100 MHz, Acetone-d_6) δ 174.85, 172.27, 158.29, 145.65, 141.33, 139.52, 137.13, 130.10, 125.06, 123.46, 121.12, 116.26, 85.21, 83.89, 77.05, 70.06, 69.76, 67.63, 62.11, 37.62, 34.18, 33.01, 30.67, 29.62, 26.06, 25.52; HRMS (ESI) calcd for $C_{36}H_{36}{}^{54}FeNO_8S$ [M - H]$^-$, 696.1593; found 696.1589.

4.2. Estrogen Receptor Binding Affinity

Relative binding affinities were determined by a competitive fluorometric binding assay as previously described. Briefly, 40 nM fluorescence tracer (coumestrol, Sigma-Aldrich, MO) and 0.8 μM purified human ERα or ERβ ligand binding domain (LBD) were diluted in 100 mM potassium phosphate buffer (pH 7.4), containing 100 μg/mL bovine gamma globulin (Sigma-Aldrich, MO). Incubations were for 2 h at room temperature (25 °C). Fluorescence polarization values were then measured. The binding affinities are expressed as relative binding affinity (RBA) values with the RBA of 17β-estradiol set to 100%. The values given are the average ± range of two independent determinations. IC_{50} values were calculated according to equations described previously.[35]

4.3. Gene Transcriptional Activity

The human embryonic kidney cell lines, HEK 293T, was maintained in Dulbecco's Minimum Essential Medium (DMEM) (Gibco by Invitrogen Corp., CA) with 10% fetal bovine serum (FBS) (Hylcone by Thermo Scientific, UT). Cells were plated in phenol red-free DMEM with 10% FBS. HEK 293T cells were transfected with 25 μL mixture per well, containing 300 ng of 3 × ERE-luciferase reporter, 100 ng of ERα or ERβ expression vector, 125 mM calcium chloride (GuoYao, China) and 12.5 μL 2 × HBS. The next day, the cells were treated with increasing doses of ER ligands diluted in phenol red-free DMEM with 10% FBS. After 24h, luciferase activity was measured using Dual-Luciferase Reporter Assay System (Promega, MI) according to the manufacturer's protocol.

4.4. HDAC Activity Assay

In vitro HDAC activity was measured using Fluorogenic HDAC6 Assay Kit (BPS Bioscience, CA) according to the manufacturer's protocol. All of the tested compounds were prepared in DMSO and were diluted in HDAC assay buffer to different concentration. The enzymatic reactions were conducted in duplicate at 37 °C for 30 min in a 50 μL mixture containing HDAC assay buffer, 5 μg of BSA, HDAC substrate, HDAC enzyme (human recombinant HDAC1, HDAC6), and various concentrations of tested compound. Then, 50 μL of 2 × HDAC Developer was added to each well and the plate was incubated at room temperature for 15 min. Fluorescence values were measured at an excitation of 350 nm and an emission of 440 nm

using SpectraMax M2 microplate reader. IC_{50} values were calculated according to the following equation using Origin software: $Y = F_b + (F_t–F_b)/(1+ 10^{[(LogIC50-X)\times Hillslope]})$, where Y = fluorescence value, F_b = minimum fluorescence value, F_t = maximum fluorescence value, X = Log [inhibitor].

4.5. Cell Culture and Cell Viability Assay

The human breast cancer cell lines MCF-7 was obtained from ATCC. DU145 and VERO cells were obtained from cell bank of Chinese Academy of Science (Shanghai, China). Cells were maintained in DMEM with 10% FBS. For all experiments, cells were grown in 96-well microtiter plates (Nest Biotech Co., China) with appropriate ligand triplicate for 72 h. MTT colormetric tests (Biosharp, China) were employed to determine cell viability per manufacturer instructions. IC_{50} values were calculated according to the following equation using Origin software: Y = 100% inhibition + (0% inhibition - 100% inhibition)/(1 + $10^{[(LogIC50-X)\times Hillslope]}$), where Y = fluorescence value, X = Log [inhibitor].[32]

4.6. Molecular Modeling

Crystal structures of ER LBD in complex with 4-hydroxytamoxifen was downloaded from the protein data bank (PDB ID: 3ERT). Compound **31b** was docked into the three-dimension structure of ERα LBD with AutoDock software (version 4.2).[48, 49] Crystallographic coordinate of the **31b** was created by Biochemoffice. The crystal structure of ERα LBD (PDB ID: 3ERD)[45] was obtained from the PDB and all water molecules were removed. Preparations of all ligands and the protein were performed with AutoDockTools (ADT). A docking cube with the edge of 60 Å, 60 Å, 58 Å in X, Y, Z dimension respectively (a grid spacing of 0.375 Å), which encompassed the whole active site, was used throughout docking. On the basis of the Lamarckian genetic algorithm (LGA), 80 runs were performed for each ligand with 500 individuals in the population.[30] The figures were prepared using PyMOL.

Acknowledgments

We are grateful to the NSFC (81573279, 81373255, 31371331), the National Basic Research Program of China (973 Program) (2012CB720600), the Key Scientific Research Projects of Ministry of Education (313040), Hubei Province's Outstanding Medical Academic Leader Program, the Fundamental Research Funds for the Central Universities of China (2015306020201), and Hunan Province Cooperative Innovation Center for Molecular Target New Drug Study for support of this research.

Supplementary data

Supplementary data associated with this article can be found, in the online version, at http://dx.doi.org/

References and Notes

1. de Deus Moura, R.; F. Carvalho, M.; Bacchi, C. E. *Breast* **2015**, 24, 461.
2. Breen, N.; Gentleman, J. F.; Schiller, J. S. *Cancer* **2011**, 117, 2209.
3. Siegel, R.; Ward, E.; Brawley, O.; Jemal, A. *CA Cancer J. Clin.* **2011**, 61, 212.
4. Brzozowski, A. M.; Pike, A. C.; Dauter, Z.; Hubbard, R. E.; Bonn, T.; Engstrom, O.; Ohman, L.; Greene, G. L.; Gustafsson, J. A.; Carlquist, M. *Nature* **1997**, 389, 753.
5. Jordan, V. C. *J. Med. Chem.* **2003**, 46, 883.
6. Jordan, V. C. *J. Med. Chem.* **2003**, 46, 1081.
7. Shang, Y.; Brown, M. *Science* **2002**, 295, 2465.
8. Jordan, V. C. *Nat. Rev. Drug. Discovery* **2003**, 2, 205.
9. Ariazi, E. A.; Ariazi, J. L.; Cordera, F.; Jordan, V. C. *Curr. Top. Med. Chem.* **2006**, 6, 181.
10. van Leeuwen, F. E.; Benraadt, J.; Coebergh, J. W.; Kiemeney, L. A.; Gimbrere, C. H.; Otter, R.; Schouten, L. J.; Damhuis, R. A.; Bontenbal, M.; Diepenhorst, F. W. *Lancet* **1994**, 343, 448.
11. Clarke, R.; Liu, M. C.; Bouker, K. B.; Gu, Z.; Lee, R. Y.; Zhu, Y.; Skaar, T. C.; Gomez, B.; O'Brien, K.; Wang, Y.; Hilakivi-Clarke, L. A. *Oncogene* **2003**, 22, 7316.
12. Irvin, W. J. J.; Carey, L. A. *Eur. J. Cancer* **2008**, 44, 2799.
13. Liu, C.; Strobl, J. S.; Bane, S.; Schilling, J. K.; McCracken, M.; Chatterjee, S. K.; Rahim-Bata, R.; Kingston, D. G. *J. Nat. Prod.* **2004**, 67, 152.
14. Ali, H.; Ahmed, N.; Tessier, G.; van Lier, J. E. *Bioorg. Med. Chem. Lett.* **2006**, 16, 317.
15. Gupta, A.; Saha, P.; Descôteaux, C.; Leblanc, V.; Asselin, E.; Bérubé, G. *Bioorg. Med. Chem. Lett.* **2010**, 20, 1614.
16. Woo, L. W.; Sutcliffe, O. B.; Bubert, C.; Grasso, A.; Chander, S. K.; Purohit, A.; Reed, M. J.; potter, B. V. *J. Med. Chem.* **2003**, 46, 3193.
17. O'Boyle, N. M.; Pollock, J. K.; Carr, M.; Knox, A. J.; Nathwani, S. M.; Wang, S.; Caboni, L.; Zisterer, D. M.; Meegan, M. J. *J. Med. Chem.* **2014**, 57, 9370.
18. Liu, J.; Flockhart, P. J.; Lu, D.; Lv, W.; Lu, W. J.; Han, X. Cushman, M.; Flockhart, D. A.; *Drug Metab. Dispos*. **2013**, 41, 1715.
19. Lv, W.; Liu, J. Z.; Lu, D.; Flockhart, D. A.; Cushman, M. J.

Med. Chem. **2013**, 56, 4611.

20. Lv, W.; Liu, J. Z.; Skaar, T. C.; Flockhart, D. A.; Cushman, M. *J. Med. Chem.* **2015**, 58, 2623.
21. Guerrant, W.; Patil, V.; Canzoneri, J. C.; Oyelere, A. K. *J. Med. Chem.* **2012**, 55, 1465.
22. Dao, K. L.; Hanson, R. N.; *Bioconjugate Chem.* **2012**, 23, 2139.
23. Li, X.; Inks, E. S.; Li, X.; Hou, J.; Chou, C. J.; Zhang, J.; Jiang, Y.; Zhang, Y.; Xu, W. *J. Med. Chem.* **2014**, 57, 3324.
24. Yang, X.; Ferguson, A. T.; Nass, S. J.; Phillips, D. L.; Butash, K. A.; Wang, S. M.; Herman, J. G.; Davidson, N. E. *Cancer Res.* **2000**, 60, 6890.
25. Yang, X. W.; Phillips, D. L.; Ferguson, A. T.; Nelson, W. G.; Herman, J. G.; Davidson, N. E. *Cancer Res.* **2001**, 61, 7025.
26. Gryder, B. E.; Rood, M. K.; Johnson, K. A.; Patil, V.; Raftery, E. D.; Yao, L. P.; Rice, M.; Azizi, B.; Doyle, D. F.; Oyelere, A. K. *J. Med. Chem.* **2013**, 56, 5782.
27. Cazares-Marinero Jde, J.; Lapierre, M.; Cavailles, V.; Saint-Fort, R.; Vessieres, A.; Top, S.; Jaouen, G. *Dalton Trans*. **2013**, 42, 15489.
28. Cazares-Marinero Jde, J.; Top, S.; Vessieres, A.; Jaouen, G. *Dalton Trans.* **2014**, 43, 817.
29. Patel, H. K.; Siklos, M. I.; Abdelkarim, H.; Mendonca, E. L.; Vaidya, A.; Petukhov, P. A.; Thatcher, G. R. *ChemMedChem* **2014**, 9, 602.
30. Zhou, H. B.; Comninos, J. S.; Stossi, F.; Katzenellenbogen, B. S.; Katzenellenbogen, J. A. *J. Med. Chem.* **2005**, 48, 7261.
31. Zheng, Y. F.; Zhu, M. H.; Srinivasan, S.; Nwachukwu, J. C.; Cavett, V.; Min, J.; Carlson, K. E.; Wang, P. C.; Dong, C.; Katzenellenbogen, J. A.; Katzenellenbogen, B. S.; Nettles, K. W.; Zhou, H. B. *ChemMedChem* **2012**, 7, 1094.
32. Zheng, Y. F.; Wang, C. H.; Li, C. H.; Qiao, J. X.; Zhang, F.; Huang, M. J.; Ren, W. M.; Dong, C.; Huang, J.; Zhou, H. B. *Org. Biomol. Chem.* **2012**, 10, 9689.
33. Zhu, M. H.; Zhang, C.; Nwachukwu, J. C.; Srinivasan, S.; Cavett, V.; Zheng, Y. F.; Carlson, K. E.; Dong, C.; Katzenellenbogen, J. A.; Nettles, K. W.; Zhou, H. B. *Org. Biomol. Chem.* **2012**, 10, 8692.
34. Wang, P. C.; Min, J.; Nwachukwu, J. C.; Cavett, V.; Carlson, K. E.; Guo, P.; Zhu, M. H.; Zheng, Y. F.; Dong, C.; Katzenellenbogen, J. A.; Nettles, K. W.; Zhou, H. B. *J. Med. Chem.* **2012**, 55, 2324.
35. Tang, C.; Li, C. H.; Zhang, S. L.; Hu, Z. Y.; Wu, J.; Dong, C.; Huang, J.; Zhou, H. B. *J. Med. Chem.* **2015**, 58, 4550.
36. Cázares Marinero, Jde. J.; Lapierre, M.; Cavaillès, V.; Saint-Fort, Vessières, R. A.; Top, S.; Jaouen, G. *Dalton Trans.* **2013**, 42, 15489.
37. van Staveren, D. R.; Metzler-Nolte, N. *Chem. Rev.* **2004**, 104, 5931.
38. Gasser, G.; Ott, I.; Metzler-Nolte, N. *J. Med. Chem.* **2011**, 54, 3.
39. Ornelas, C. *N. J. Chem.* **2011**, 35, 1973.
40. Top, S.; Vessieres, A.; Leclercq, G.; Quivy, J.; Tang, J.; Vaissermann, J.; Huche, M.; Jaouen, G. *Chemistry* **2003**, 9, 5223.
41. Vessières, A.; Top, S.; Pigeon, P.; Hillard, E.; Boubeker, L.; Spera, D.; Jaouen, G. *J. Med. Chem.* **2005**, 48, 3937.
42. Nguyen, A.; Top, S.; Pigeon, P.; Vessieres, A.; Hillard, E. A.; Plamont, M. A.; Huche, M.; Rigamonti, C.; Jaouen, G. *Chemistry* **2009**, 15, 684.
43. Plazuk, D.; Vessieres, A.; Hillard, E. A.; Buriez, O.; Labbe, E.; Pigeon, P.; Plamont, M. A.; Amatore, C.; Zakrzewski, J.; Jaouen, G. *J. Med. Chem.* **2009**, 52, 4964.
44. Oger, F.; Lecorgne, A.; Sala, E.; Nardese, V.; Demay, F.; Chevance, S.; Desravines, D. C.; Aleksandrova, N.; Guével, R. L.; Lorenzi, S.; Beccari, A. R.; Barath, P.; Hart, D. J.; Bondon, A.; Carettoni, D.; Simonneaux, G.; Salbert, G. *J. Med. Chem.* **2010**, 53, 1937.
45. Shiau, A. K.; Barstad, D.; Loria, P. M.; Cheng, L.; Kushner, P. J.; Agard, D. A.; Greene, G. L. *Cell* **1998**, 95, 927.
46. Park, S. Y.; Jun, J. A.; Jeong, K. J.; Heo, H. J.; Sohn, J. S.; Lee, H. Y.; Park, C. G.; Kang, J. *Oncol. Rep.* **2011**, 25, 1677.
47. Biggins, J. B.; Koh, J. T. *Curr. Opin. Chem. Biol.* **2007**, 11, 99.
48. Huey, R.; Morris, G. M.; Olson, A. J.; Goodsell, D. S. *J. Comput. Chem.* **2007**, 28, 1145.
49. Audie, J. *Biophys. Chem.* **2009**, 139, 84.

Synthesis and structure-activity relationships of novel hybrid ferrocenyl compounds based on a bicyclic core skeleton for breast cancer therapy

Changhao Li [a], Chu Tang [b], Zhiye Hu [b], Chenxi Zhao [a], Chenlu Li [b], Silong Zhang [b], Chune Dong [b], Hai-Bing Zhou [b,*], Jian Huang [a,*]

Incorporation of the ferrocenyl group into OBHS-HDACi skeleton could lead to FcOBHS-HDACi complexes, which show significant antiproliferative effect on both ER(+) and ER(-) breast cancer cells.